Supporting Information

Fused Pyrazolo[3,4-*d*]pyridazine *N*-Oxides with Balanced Detonation Performance and Safety

Congcong Li [a,b], Hongquan Yin [a], Qing Ma *[c], Fu-Xue Chen *[a]

[a] School of Chemistry & Chemical Engineering, Beijing Institute of Technology, Beijing 102488, China.

[b] College of Chemistry, Chemical Engineering and Materials Science, Zaozhuang University, Zaozhuang 277160, China.

[c] National Key Laboratory of Chemical Explosion Safety, Institute of Chemical Materials, China Academy of Engineering Physics, Mianyang 621900, China.

* Corresponding authors. Email addresses: qingma@caep.cn(Q. Ma), fuxue.chen@bit.edu.cn (F.-X. Chen)

Table of Contents

1. Theoretical calculations

1.1. Heat of formation

Highly accurate composite ab initio methods and density functional theory (DFT) calculations were carried out with the Gaussian 09 programs.[S1] The enthalpy (*H*) for compound at standard condition (298K, 1atm) were directly calculated by G4(MP2)-6x method.[S2] Geometries were optimized with the M06-2X functional using the 6-31+G(2df, p) basis set.[S3] Single-point energies were obtained at the HF, MP2, and CCSD(T) levels for the composite procedures. Zero-point vibrational energies (ZPVEs) and thermal corrections to enthalpy (ΔH) at 298K, derived from scaled M06-2X/6-31+G(2df, p) frequencies, were incorporated into the total energies.

After acquiring the enthalpy of compounds, their gas phase enthalpy of formation can be calculated by atomization method as following Equation (1):

$$\Delta H_f(g) = H(\mathrm{C_aH_bO_cN_d}) - aH(\mathrm{C(g)}) - \frac{b}{2}H(\mathrm{H_2(g)}) - \frac{c}{2}H(\mathrm{O_2(g)}) - \frac{d}{2}H(\mathrm{N_2(g)}) + aH_{vap}(\mathrm{graphite}) \qquad (1)$$

The final solid phase heat of formation was obtained by subtracting the corrected value of the decomposition temperature from the calculated gas phase enthalpy of formation. The heat of formation of compound **2** in the standard state (298K, 1atm) are given directly in the following Table S1.

Table S1 Heat of formation for the compounds

Compound	ΔH_f (**kJ mol^{-1}**)
2	189.7

1.2. Heat of formation

All computational calculations were performed using the Gaussian 16 (C01) software package. DFT calculations were conducted employing Becke's three-parameter hybrid exchange functional combined with the Lee–Yang–Parr correlation functional (B3LYP)[S4], incorporating Grimme's D3 dispersion correction with Becke–Johnson damping (DFT-D3BJ).[S5] Geometry optimization and subsequent frequency analysis were carried out at the def2-SVP basis set level. Frequency calculations verified the absence of imaginary frequencies, confirming that all optimized molecular structures corresponded to stable minima on the potential energy surface. Single-point energy calculations were further implemented using the higher-precision def2-TZVP basis set.[S6] The Fukui function diagrams were visualized via the combined application of Multiwfn and VMD software.

The f^- Fukui function characterizes oxidation activity (Fig. S1). N11 possesses the largest f^- value (0.1002) and is the dominant reactive site, while N9 (0.0818), N10 (0.0865) and N7 (0.0614) exhibit lower activity. Conjugation in the five-membered ring increases the electron density and f^- value of N7 Oxidation of N11 yields an N-oxide, which forms intramolecular hydrogen bonds with N9. This reduces the electron density and reactivity of N9, N7 and N10 are sterically accessible for oxidant attack, whereas the N11 oxide group shields the N9 site. Additionally, hydrogen bonding stabilizes N9 and stops further oxidation. In summary, the combined effects of intrinsic reactivity, hydrogen bonding, steric hindrance and conjugation lead to the selective oxidation.

Fukui Function

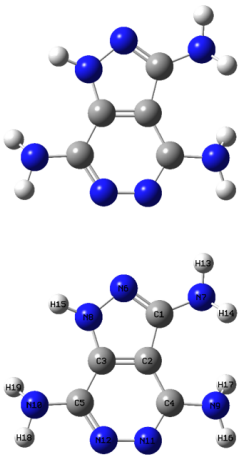

Atom	q(N)	q(N+1)	q(N-1)	f-	f+	f0	CDD
1(C)	0.0698	0.0117	0.1138	0.044	0.0581	0.051	0.0141
2(C)	-0.058	-0.1162	-0.0413	0.0167	0.0583	0.0375	0.0416
3(C)	0.0213	-0.0311	0.0395	0.0182	0.0524	0.0353	0.0341
4(C)	0.0818	0.0333	0.1358	0.054	0.0485	0.0512	-0.0055
5(C)	0.0694	-0.0123	0.1326	0.0631	0.0817	0.0724	0.0186
6(N)	-0.1733	-0.2835	-0.0988	0.0745	0.1102	0.0924	0.0356
7(N)	-0.1698	-0.2051	-0.1084	0.0614	0.0353	0.0483	-0.0261
8(N)	-0.0199	-0.0762	0.0456	0.0655	0.0563	0.0609	-0.0092
9(N)	-0.1682	-0.2043	-0.0864	0.0818	0.0362	0.059	-0.0456
10(N)	-0.1789	-0.2229	-0.0924	0.0865	0.044	0.0652	-0.0426
11(N)	-0.1643	-0.2212	-0.0641	0.1002	0.057	0.0786	-0.0432
12(N)	-0.1462	-0.2664	-0.0666	0.0796	0.1202	0.0999	0.0406
13(H)	0.1209	0.0869	0.1552	0.0343	0.0339	0.0341	-0.0004
14(H)	0.1145	0.0896	0.1413	0.0268	0.0249	0.0259	-0.0019
15(H)	0.147	0.1064	0.1823	0.0353	0.0405	0.0379	0.0052
16(H)	0.1171	0.0832	0.1565	0.0393	0.0339	0.0366	-0.0054
17(H)	0.1119	0.0817	0.1483	0.0364	0.0302	0.0333	-0.0062
18(H)	0.1153	0.0754	0.1551	0.0398	0.0399	0.0399	0.0001
19(H)	0.1099	0.0712	0.1523	0.0425	0.0387	0.0406	-0.0038

Figure S1 Fukui function distributions of compound **1**.

1.3. Reference

[S1] Frisch, M. J.; Trucks, G. W.; Schlegel, H. B.; Scuseria, G. E.; Robb, M. A.; Cheeseman, J. R.; Scalmani, G.; Barone, V.; Mennucci, B.; Petersson, G. A.; Nakatsuji, H.; Caricato, M.; Li, X.; Hratchian, H. P.; Izmaylov, A. F.; Bloino, J.; Zheng, G.; Sonnenberg, J. L.; Hada, M.; Ehara, M.; Toyota, K.; Fukuda, R.; Hasegawa, J.; Ishida, M.; Nakajima, T.; Honda, Y.; Kitao, O.; Nakai, H.; Vreven, T.; Montgomery, J. A., Jr; Peralta, J. E.; Ogliaro, F.; Bearpark, M.; Heyd, J. J.; Brothers, E.; Kudin, K. N.; Staroverov, V. N.; Keith, T.; Kobayashi, R.; Normand, J.; Raghavachari, K.; Rendell, A.; Burant, J. C.; Iyengar, S. S.; Tomasi, J.; Cossi, M.; Rega, N.; Millam, J. M.; Klene, M.; Knox, J. E.; Cross, J. B.; Bakken, V.; Adamo, C.; Jaramillo, J.; Gomperts, R.; Stratmann, R. E.; Yazyev, O.; Austin, A. J.; Cammi, R.; Pomelli, C.; Ochterski, J. W.; Martin, R. L.; Morokuma, K.; Zakrzewski, V. G.; Voth, G. A.; Salvador, P.; Dannenberg, J. J.; Dapprich, S.; Daniels, A. D.; Farkas, O.; Foresman, J. B.; Ortiz, J. V.; Cioslowski, J.; Fox, D. J. Gaussian 09, Revision B. 01; Gaussian, Inc.: Wallingford, CT, **2009**.

[S2] Chan, B.; Deng, J.; Radom, L. G4(MP2)-6X: A Cost-Effective Improvement to G4(MP2). *J. Chem. Theory Comput.* **2010**, *7*, 112–120.

[S3] Zhao, Y.; Truhlar, D. G. The M06 Suite of Density Functionals for Main Group Thermochemistry, Thermochemical Kinetics, Noncovalent Interactions, Excited States, and Transition Elements: Two New Functionals and Systematic Testing of Four M06-Class Functionals and 12 Other Functionals. *Theor. Chem. Acc.* **2007**, *120*, 215–241.

[S4] Adamo C., Barone V. Toward reliable density functional methods without adjustable parameters: The PBE0 model. *J. Chem. Phys*. **1999**, 110, 6158-6170.

[S5] Grimme S, Ehrlich S, Goerigk L. Effect of the damping function in dispersion corrected density functional theory. *J Comput Chem*. **2011**, 32, 1456-65.

[S6] Weigend F.; Ahlrichs, R., Balanced basis sets of split valence, triple zeta valence and quadruple zeta valence quality for H to Rn: Design and assessment of accuracy. *Phys. Chem. Chem. Phys*. **2005**, 7, 3297.

2. Experimental section

2.1. Safety Precaution!

Although we have not experienced any difficulties in handling these new energetic materials, small scale and best safety practices (leather gloves, face shield, and safety glasses) are strongly encouraged. All compounds should be handled with care using the best safety practices.

2.2. Characterization methods

^{1}H NMR and ^{13}C NMR spectra were recorded on a Bruker Avance 400 spectrometer operating at 400 and 100 MHz, respectively. Decomposition temperatures were measured using a Shimadzu TA-60ws differential scanning calorimeter (DSC) at a heating rate of 10 °C min^{-1} under an argon atmosphere. IR spectra were recorded on a Bruker ALPHA FT-IR spectrometer using KBr pellets. High-resolution mass spectra (HRMS) were obtained on a Bruker Apex IV FTMS instrument. Impact and friction sensitivities were determined using a standard BAM Fallhammer and a BAM friction tester, respectively. Detonation velocity and pressure were calculated using the EXPLO5 (version 6.02) software package. X-Ray diffractions of all single crystals were carried out on a Bruker D8 VENTURE diffractometer using Mo-Kα radiation (λ = 0.71073 Å). The crystal was kept at 296.15 K during data collection. Data reduction, structure solution and refinement were performed using the Olex2 software package.

2.3. Synthetic procedures

2.3.1. *Synthesis of 1H-Pyrazolo[3,4-d]pyridazine-3,4,7-triamine (1).*

Hydrazine hydrate (80%, 0.8 mL, 20 mmol) was added dropwise to a stirred solution of 5-amino-1*H*-pyrazole-3,4-dicarbonitrile (0.500 g, 3.75 mmol) in 50% acetic acid (2.0 mL) at 25 °C. The reaction mixture was heated at 80 °C for 4 h. The precipitate was collected by filtration and washed with distilled water (3.0 mL) to afford compound **1** as a white solid (0.250 g, 40 %). ^{1}H NMR (400 MHz, DMSO-*d6*): δ = 8.44 (s, 2H, NH_2), 6.54 (s, 4H, NH_2) ppm; ^{13}C{H} NMR (100 MHz, DMSO-d6): δ_C = 149.8 (s, 1C), 149.3 (s, 1C), 146.1 (s, 1C), 136.3 (s, 1C), 92.9 (s, 1C) ppm; IR (KBr): ν = 3311 (w), 3115 (w), 1689 (w), 1627 (s), 1508 (s), 1458 (s), 1361 (m), 1099 (w), 1045 (w), 756 (s) cm^{-1}; HRMS (ESI-TOF) *m/z*: $[M + H]^+$ Calc. for $C_5H_8N_7$ 166.0836; Found 166.0826.

2.3.2. *Synthesis of 4-amino-3,7-dinitro-1H-pyrazolo[3,4-d]pyridazine-5-oxide (2)*

Compound **1** (0.165 g, 1.0 mmol) was dispersed in 30% H_2O_2 (2.0 mL), and 98% concentrated sulfuric acid (2.0 mL) was added dropwise at 0 °C. Then Na_2WO_4 (1.0 mmol, 0.330 g) was added in batches and the reaction mixture was stirred for additional 5 h at room temperature. The reaction process was monitored by thin layer chromatography. After the reaction

was completed, the reaction mixture was poured into 15.0 mL ice water and extracted with ethyl acetate (10.0 mL × 3). The organic layers were combined and washed followed by water (10.0 mL × 3) and brine, then dried over anhydrous sodium sulfate. Compound **2** (0.082 g, 36 %) was isolated as red-brown crystals by column chromatography (methanol/dichloromethane = 1:20, v/v). ^{1}H NMR (400 MHz, DMSO-*d6*): δ = 9.28 (s, 1H, NH_2) ppm, δ = 7.76 (s, 1H, NH_2) ppm; ^{13}C {H}NMR (100 MHz, DMSO-*d6*): δ_C = 150.0 (s, 1C), 149.8 (s, 1C), 144.9 (s, 1C), 133.8 (s, 1C), 97.7 (s, 1C) ppm; IR (KBr): ν =3566 (s), 3443 (s), 1645 (s), 1537 (s), 1387 (m), 1285 (m), 1175 (s), 970 (s) cm^{-1}; HRMS (ESI-TOF) *m/z*: $[M - H]^-$ Calc. for $C_5H_2N_7O_5^-$: 240.0122, Found: 240.0123.

3. Crystallographic data

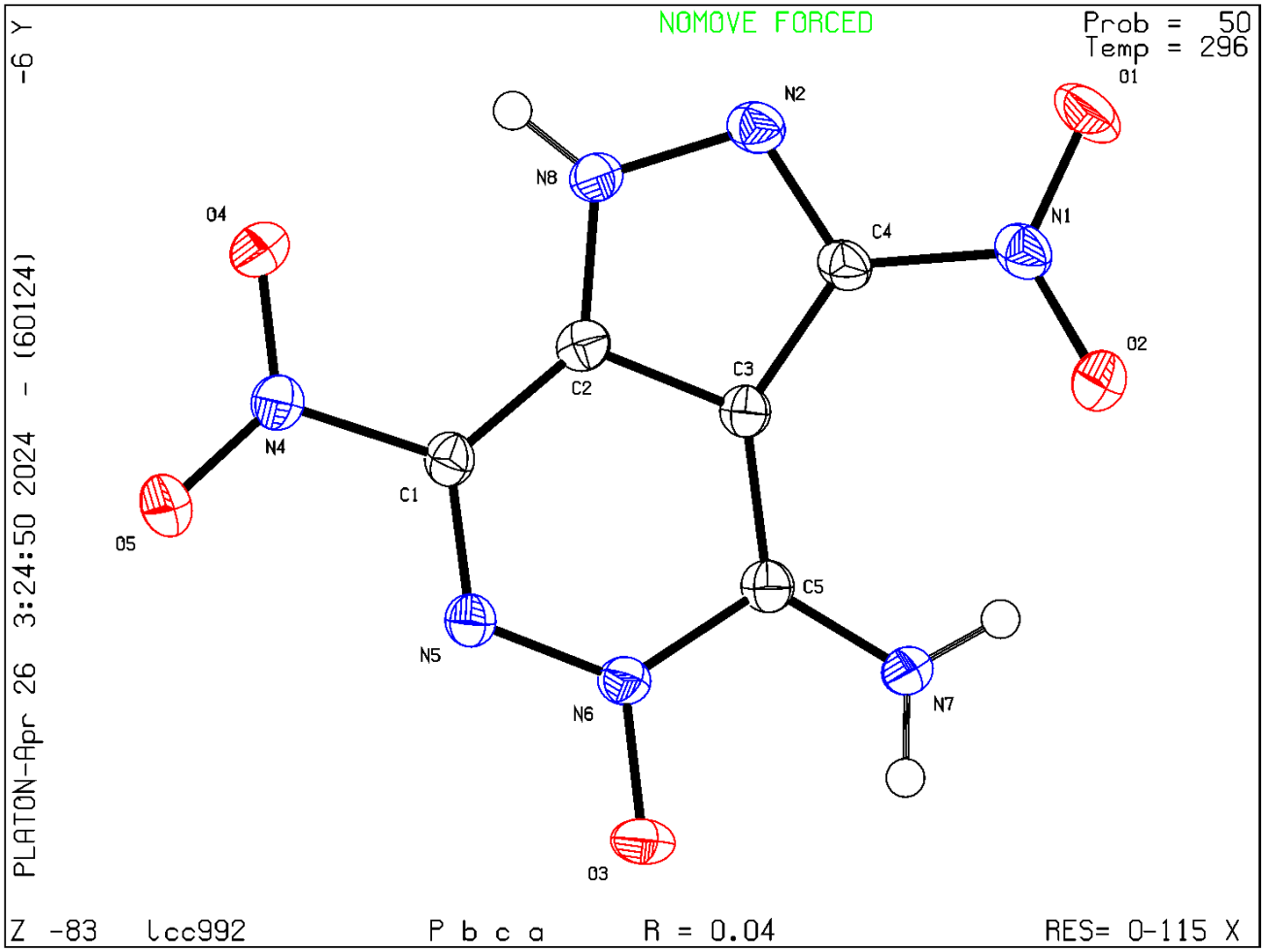

Figure S2 Crystal structures of compound **2**.

Table S2 Crystal data and structure refinement for compound **2**.

Compound	**2** (CCDC: 2357665)
Empirical formula	$C_5H_3N_7O_5$
Formula weight	241.14
Temperature	296.15 K
Crystal system	Orthorhombic
Space group	*Pbca*
a[Å]	13.9980(17)
b[Å]	6.7180(9)
c[Å]	17.197(2)
α[°]	90
β[°]	90
γ[°]	90
Volume	1617.2(3) Å^3

Z	8
Density	1.981 g/m^3
F(000)	976.0
Crystal size	0.220 x 0.200 x 0.150 mm^3
Theta range for data collection	10.504 to 113.76°
Index ranges	-17≤h≤15, -8≤k≤8, -20≤l≤21
Reflections collected	11932
Independent reflections	1644 [R(int) = 0.0491]
Data / restraints / parameters	1644 / 0 / 155
Goodness-of-fit on F^2	1.065
Final R indices [I>2sigma(I)]	R1 = 0.0351, wR2 = 0.0879
R indices (all data)	R1 = 0.0398, wR2 = 0.0908
Largest diff. peak and hole	0.34 and -0.24 e.Å^{-3}

Table S3 Fractional Atomic Coordinates (×10^4) and equivalent isotropic displacement parameters (Å^2×10^3) for compound **2.** U_{eq} is defined as 1/3 of the trace of the orthogonalized U_{ij} tensor.

Atom	***x***	***y***	***z***	**U(eq)**
O4	4567.2(8)	-8789.0(19)	-6107.1(7)	26.3(3)
O2	4410.6(8)	-4046(2)	-2592.9(7)	28.6(3)
O3	1485.1(8)	-6883.2(19)	-4106.3(7)	26.3(3)
O1	5939.9(8)	-4440(2)	-2755.4(7)	30.6(3)
O5	3047.2(9)	-9316(2)	-6322.2(7)	34.1(4)
N6	2389.8(9)	-7065(2)	-4273.2(7)	19.0(3)
N8	5228.3(9)	-7159(2)	-4729.2(8)	19.1(3)
N5	2618.7(9)	-7815(2)	-4962.8(7)	19.2(3)
N7	2663.7(9)	-5822(2)	-3058.5(8)	21.7(3)
N1	5105.9(10)	-4729(2)	-2940.0(8)	21.9(3)
N4	3713.8(10)	-8757(2)	-5920.8(8)	21.6(3)
N2	5624.7(9)	-6274(2)	-4105.7(8)	20.6(3)
C1	3521.3(11)	-7954(2)	-5150.5(9)	18.0(4)
C3	4011.4(11)	-6482(2)	-3937.6(9)	17.3(3)
C4	4909.3(11)	-5871(2)	-3636.0(9)	18.4(4)
C2	4266.2(11)	-7301(2)	-4659.0(9)	17.5(3)
C5	3036.3(11)	-6427(2)	-3718.4(9)	18.2(4)

Table S4 Bond lengths [Å] and angles [°] for compound **2**.

Bond	Bond lengths [Å]	Bond	Bond lengths [Å]
O(4)-N(4)	1.237(18)	N(5)-C(1)	1.307(2)
O(2)-N(1)	1.230(18)	N(7)-C(5)	1.313(2)
O(3)-N(6)	1.304(17)	N(1)-C(4)	1.448(2)

O(1)-N(1)	1.225(18)	N(4)-C(1)	1.456(2)
O(5)-N(4)	1.219(18)	N(2)-C(4)	1.315(2)
N(6)-N(5)	1.327(18)	C(1)-C(2)	1.412(2)
N(6)-C(5)	1.383 (2)	C(3)-C(4)	1.420(2)
N(8)-N(2)	1.345(19)	C(3)-C(2)	1.403(2)
N(8)-C(2)	1.355(19)	C(3)-C(5)	1.416(2)

Table S5 Bond angles [ ] for compound **2**.

Bond	Bond angles [°]	Bond	Bond angles [°]
O3-N6-N5	117.80(12)	C2-C1-N4	121.54(14)
O3-N6-C5	117.03(13)	C2-C3-C4	102.20(13)
N5-N6-C5	125.16(13)	C2-C3-C5	119.37(14)
N2-N8-C2	111.71(13)	C5-C3-C4	138.42(15)
C1-N5-N6	118.73(13)	N2-C4-N1	118.18(13)
O2-N1-C4	116.63(13)	N2-C4-C3	112.96(14)
O1-N1-O2	124.67(14)	C3-C4-N1	128.55(14)
O1-N1-C4	118.63(14)	N8-C2-C1	134.61(15)
O4-N4-C1	114.89(13)	N8-C2-C3	107.67(14)
O5-N4-O4	125.94(14)	C3-C2-C1	117.59(14)
O5-N4-C1	119.18(13)	N6-C5-C3	116.03(14)
C4-N2-N8	105.45(13)	N7-C5-N6	115.60(14)
N5-C1-N4	115.46(13)	N7-C5-C3	128.36(15)

Table S6 Torsion angles [ ] for compound **2**.

Torsion	angles [°]	Torsion	angles [°]
O4-N4-C1-N5	176.56(14)	N4-C1-C2-N8	2.3(3)
O4-N4-C1-C2	-1.0(2)	N4-C1-C2-C3	177.77(14)
O2-N1-C4-N2	166.31(15)	N2-N8-C2-C1	174.88(17)
O2-N1-C4-C3	-6.7(2)	N2-N8-C2-C3	-0.86(18)
O3-N6-N5-C1	177.96(14)	C4-C3-C2-N8	0.77(17)
O3-N6-C5-N7	4.3(2)	C4-C3-C2-C1	-175.82(14)
O3-N6-C5-C3	-174.85(14)	C4-C3-C5-N6	173.25(18)
O1-N1-C4-N2	-10.8(2)	C4-C3-C5-N7	-5.8(3)
O1-N1-C4-C3	176.19(16)	C4-N8-N2-C4	0.55(18)
O5-N4-C1-N5	-3.0(2)	C2-C3-C4-N1	172.89(15)
O5-N4-C1-C2	179.44(15)	C2-C3-C4-N2	-0.47(18)
N6-N5-C1-N4	-178.96(13)	C2-C3-C5-N6	-4.9(2)
N6-N5-C1-C2	-1.4(2)	C2-C3-C5-N7	176.14(16)
N8-N2-C4-N1	-174.13(13)	C5-N6-N5-C1	-0.9(2)
N8-N2-C4-C3	-0.03(18)	C5-C3-C4-N1	-5.4(3)
N5-N6-C5-N7	-176.82(14)	C5-C3-C4-N2	-178.77(19)
N5-N6-C5-C3	4.0(2)	C5-C3-C2-N8	179.48(14)
N5-C1-C2-N8	-175.08(17)	C5-C3-C2-C1	2.9(2)

Table S7 Anisotropic displacement parameters ($Å^2 \times 10^3$) for compound **2**. The anisotropic displacement factor exponent takes the form:

$-2\pi^2[h^2 a^{*2}U_{11} + ... + 2hka^* b^* U_{12}]$

Atom	**U_{11}**	**U_{22}**	**U_{33}**	**U_{23}**	**U_{13}**	**U_{12}**
O4	21.5(6)	35.2(7)	22.2(6)	-2.6(5)	4.2(5)	0.4(5)
O2	26.0(6)	40.4(8)	19.4(6)	-4.5(5)	2.9(5)	-4.3(5)
O3	13.5(6)	39.2(8)	26.4(6)	-0.6(5)	0.4(4)	-0.8(5)
O1	20.1(6)	40.9(8)	30.7(7)	-0.4(6)	-11.2(5)	-3.8(5)
O5	25.7(7)	55.6(9)	20.9(6)	-10.2(6)	-2.8(5)	-6.1(6)
N6	15.3(6)	25.1(8)	16.4(6)	1.3(5)	-0.3(5)	0.1(5)
N8	16.1(6)	24.1(8)	17.0(6)	0.6(6)	0.9(5)	1.5(5)
N5	18.8(7)	23.2(8)	15.6(6)	0.8(5)	-0.7(5)	-0.7(5)
N7	15.9(7)	32.4(8)	16.9(7)	-2.9(6)	1.0(5)	0.5(6)
N1	20.1(7)	27.8(8)	17.7(7)	4.4(6)	-3.3(5)	-2.8(6)
N4	20.7(7)	27.6(8)	16.6(7)	0.3(6)	0.3(5)	-0.7(6)
N2	17.2(7)	25.4(8)	19.3(7)	3.6(6)	-1.5(5)	-0.1(5)
C1	19.9(8)	19.8(8)	14.3(7)	1.7(6)	-0.7(6)	0.0(6)
C3	18.1(8)	19.5(8)	14.2(7)	3.0(6)	-0.8(6)	0.1(6)
C4	16.4(7)	22.6(8)	16.2(8)	3.6(6)	-2.6(6)	-0.5(6)
C2	17.8(7)	18.4(8)	16.2(7)	3.5(6)	0.8(6)	1.5(6)
C5	18.3(8)	19.8(8)	16.4(7)	2.7(6)	-0.9(6)	0.5(6)

Table S8 Hydrogen coordinates ($\times 10^4$) and isotropic displacement parameters ($Å^2 \times 10^3$) for compound **2**.

Atom	***x***	***y***	***z***	**U(eq)**
H8	5546.39	-7582.42	-5123.73	23
H7A	2054.46	-5841.32	-2994.42	26
H7B	3028.95	-5407.69	-2690.49	26

4. Copies of spectra of compounds

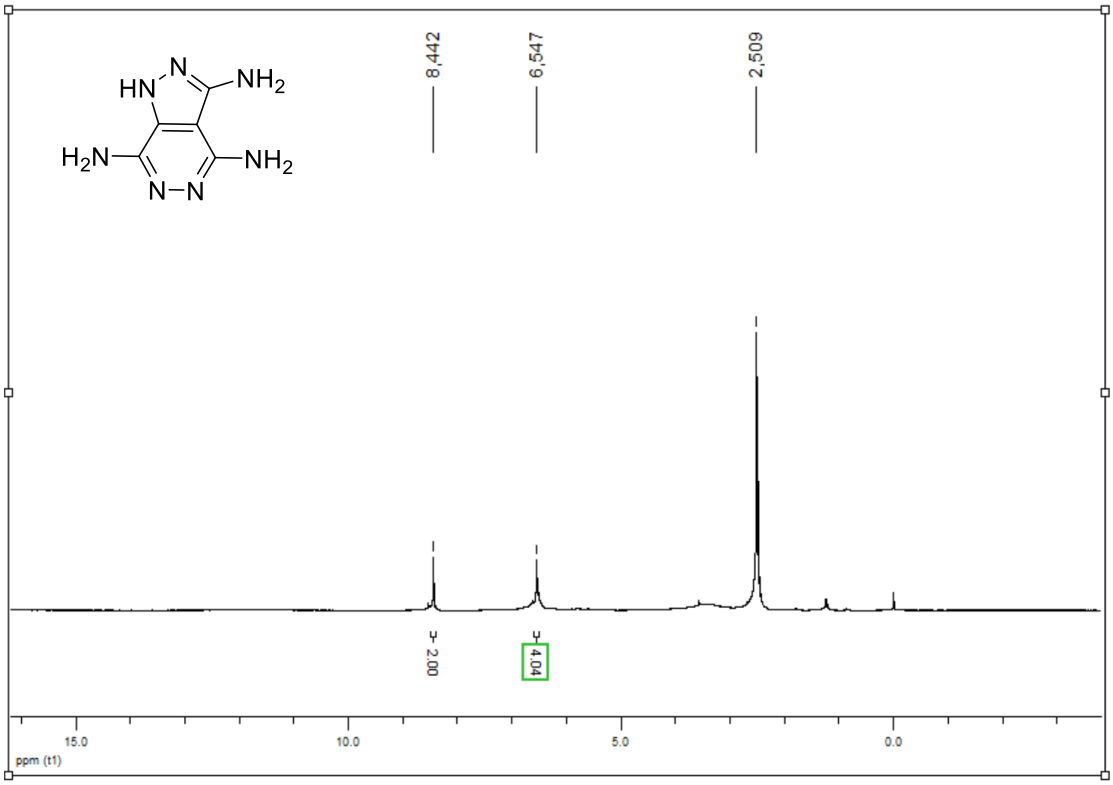

Figure S3 ^{1}H NMR spectrum of **1**.

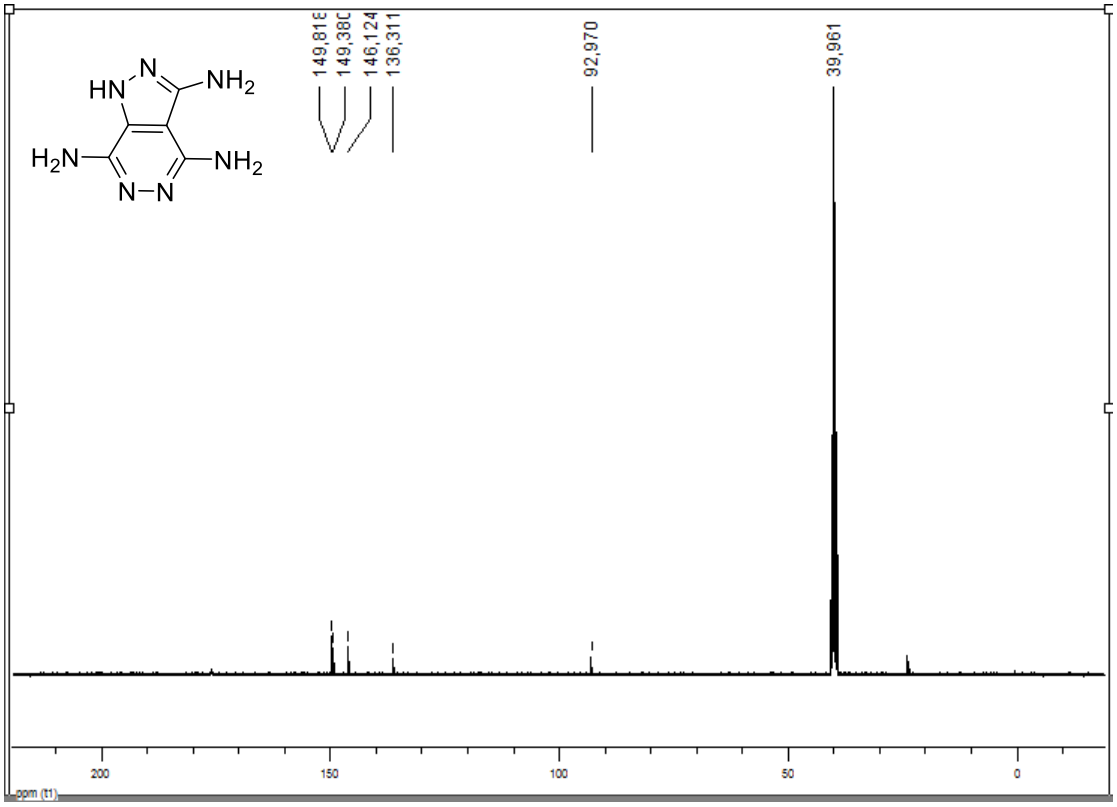

Figure S4 ^{13}C NMR spectrum of **1**.

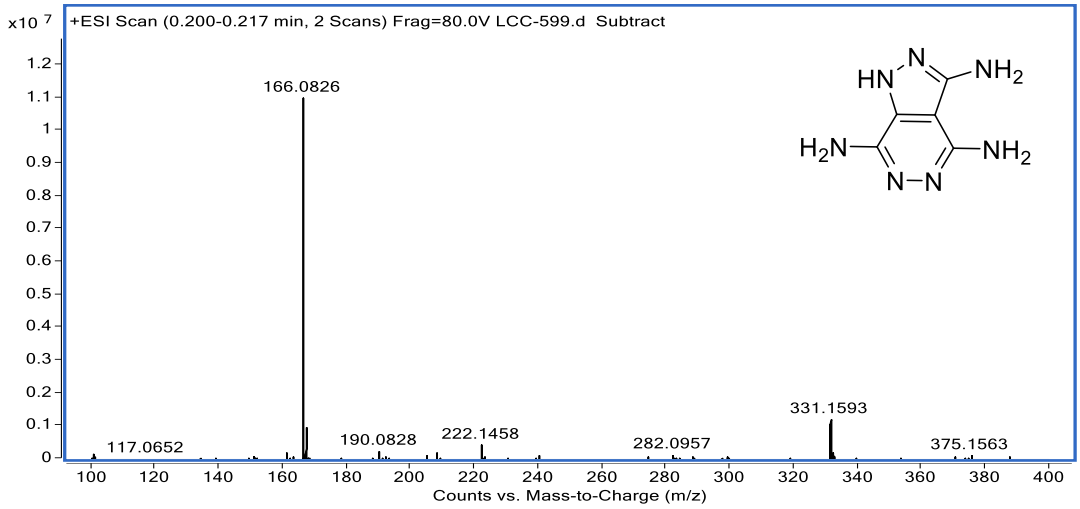

Figure S5 ESI-HRMS spectrum of **1**.

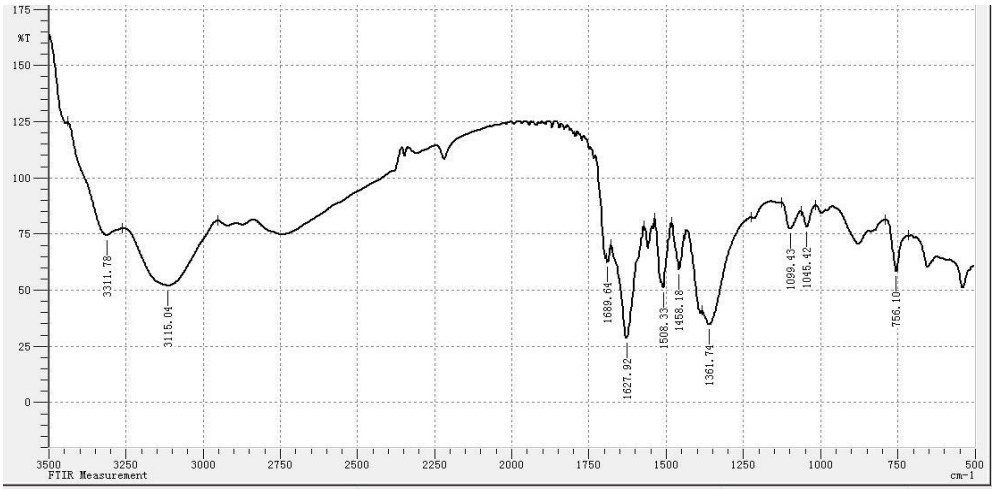

Figure S6 IR spectrum of **1**.

Figure S7 ^{1}H NMR spectrum of **2**.

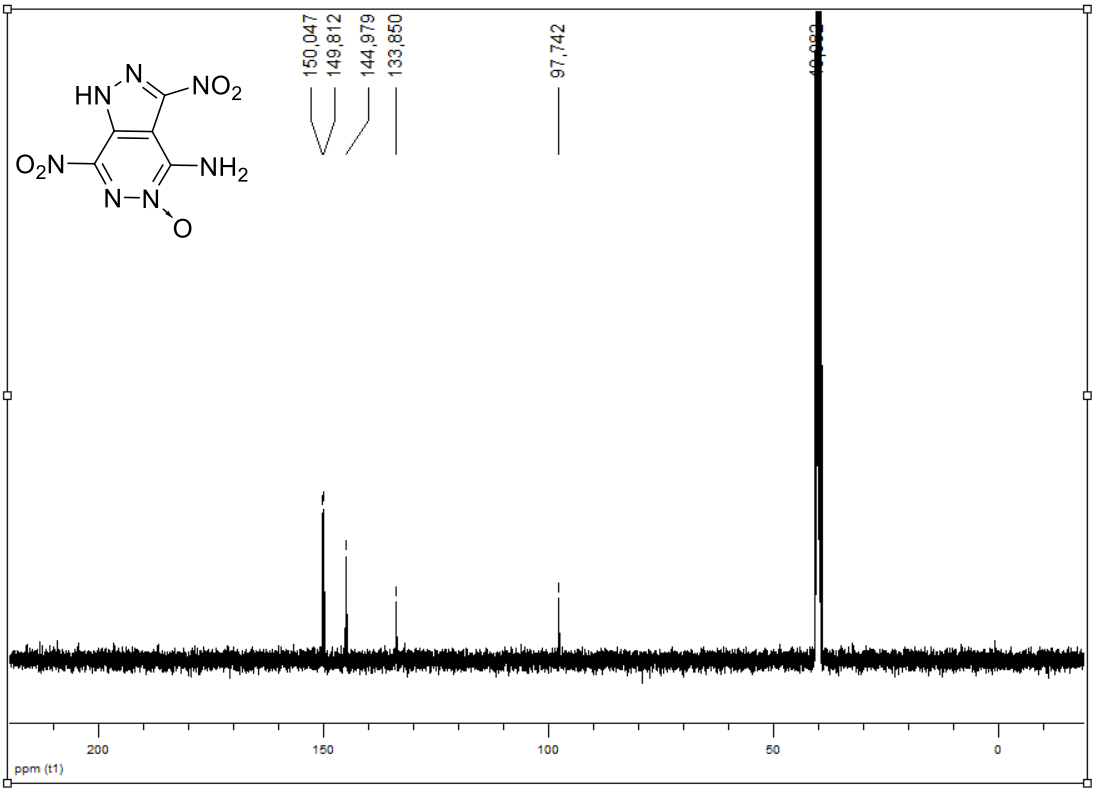

Figure S8 ^{13}C NMR spectrum of **2**.

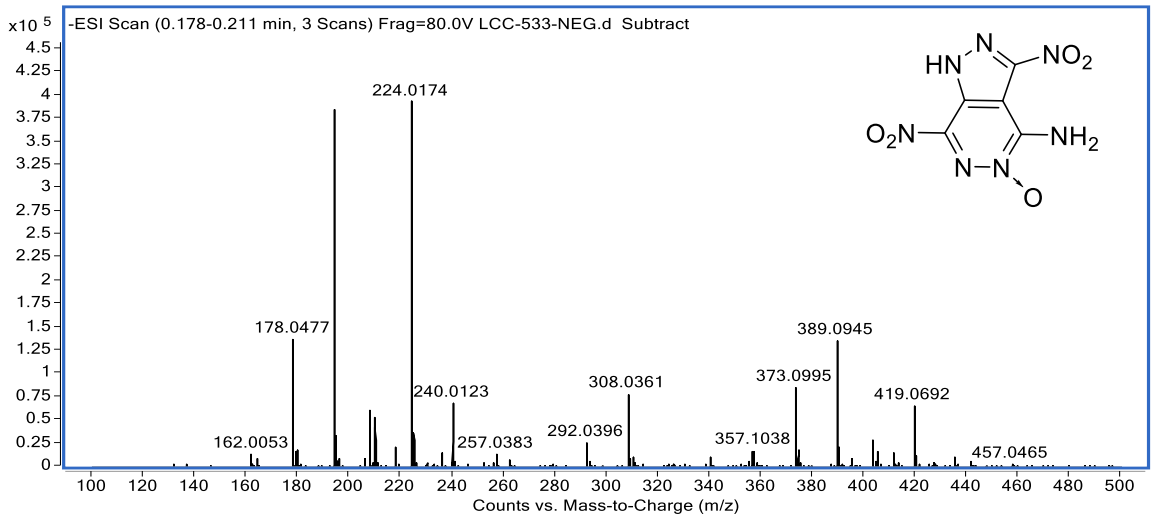

Figure S9 ESI-HRMS spectrum of **2**.

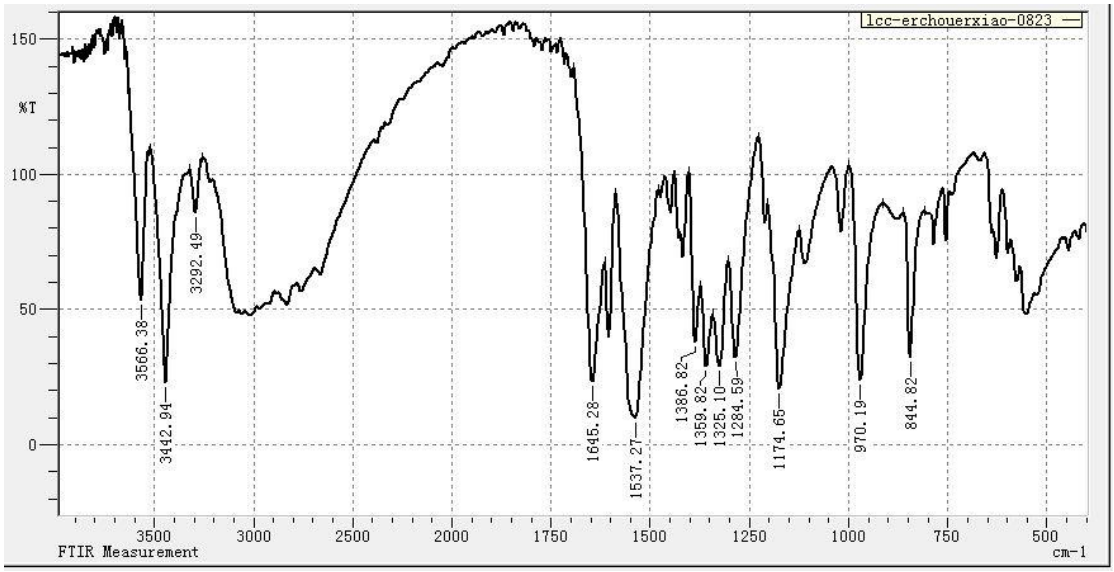

Figure S10 IR spectrum of **2**.

5. DSC curve of energetic compound 2

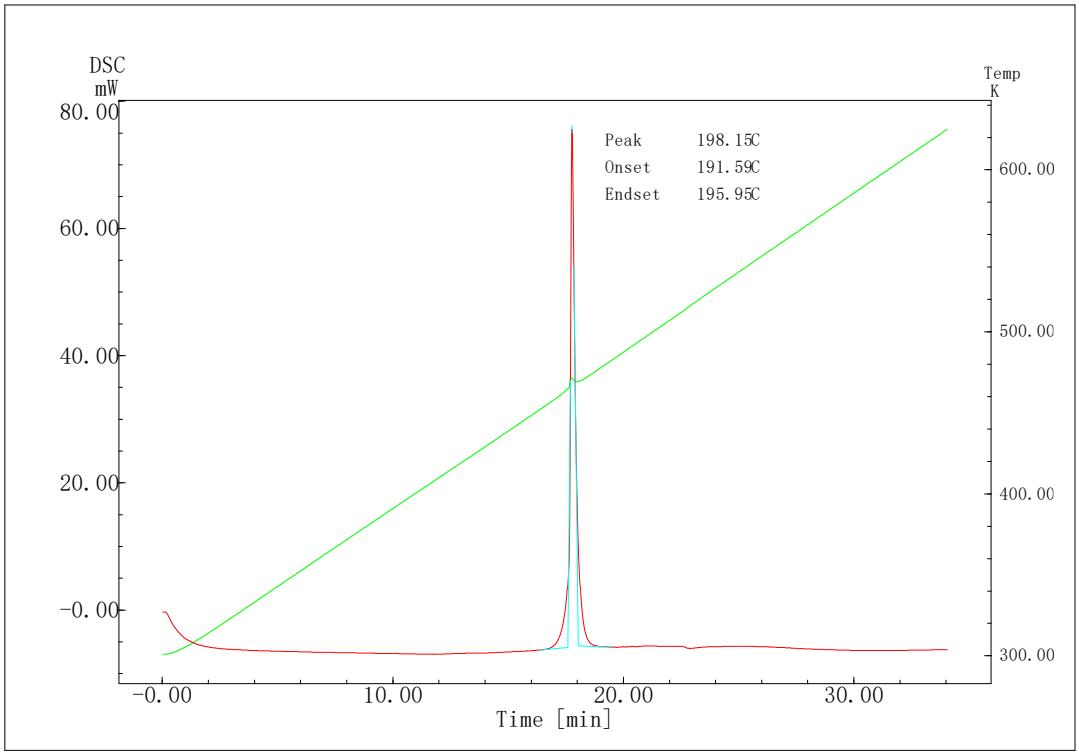

Figure S11 DSC curve of **2**.